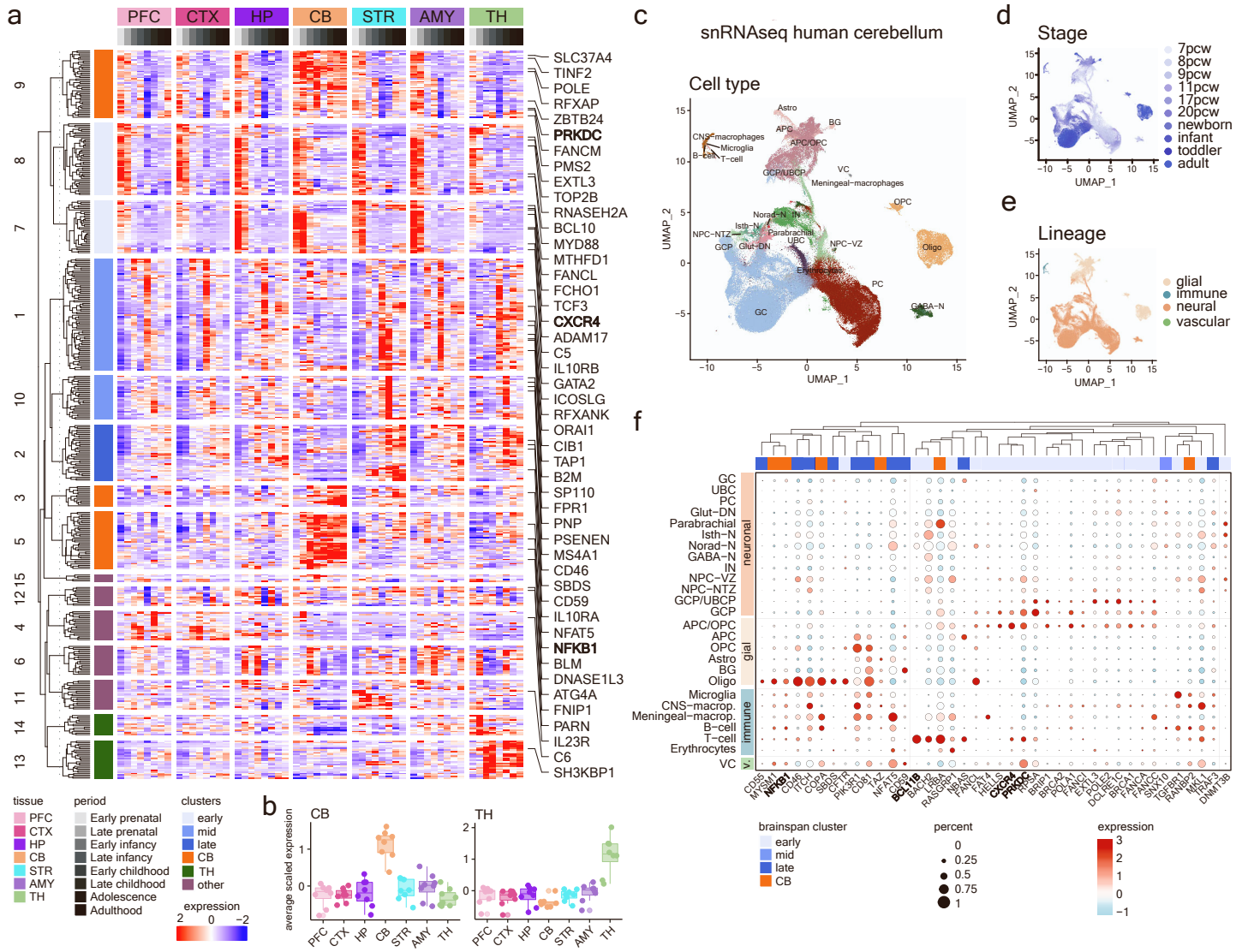
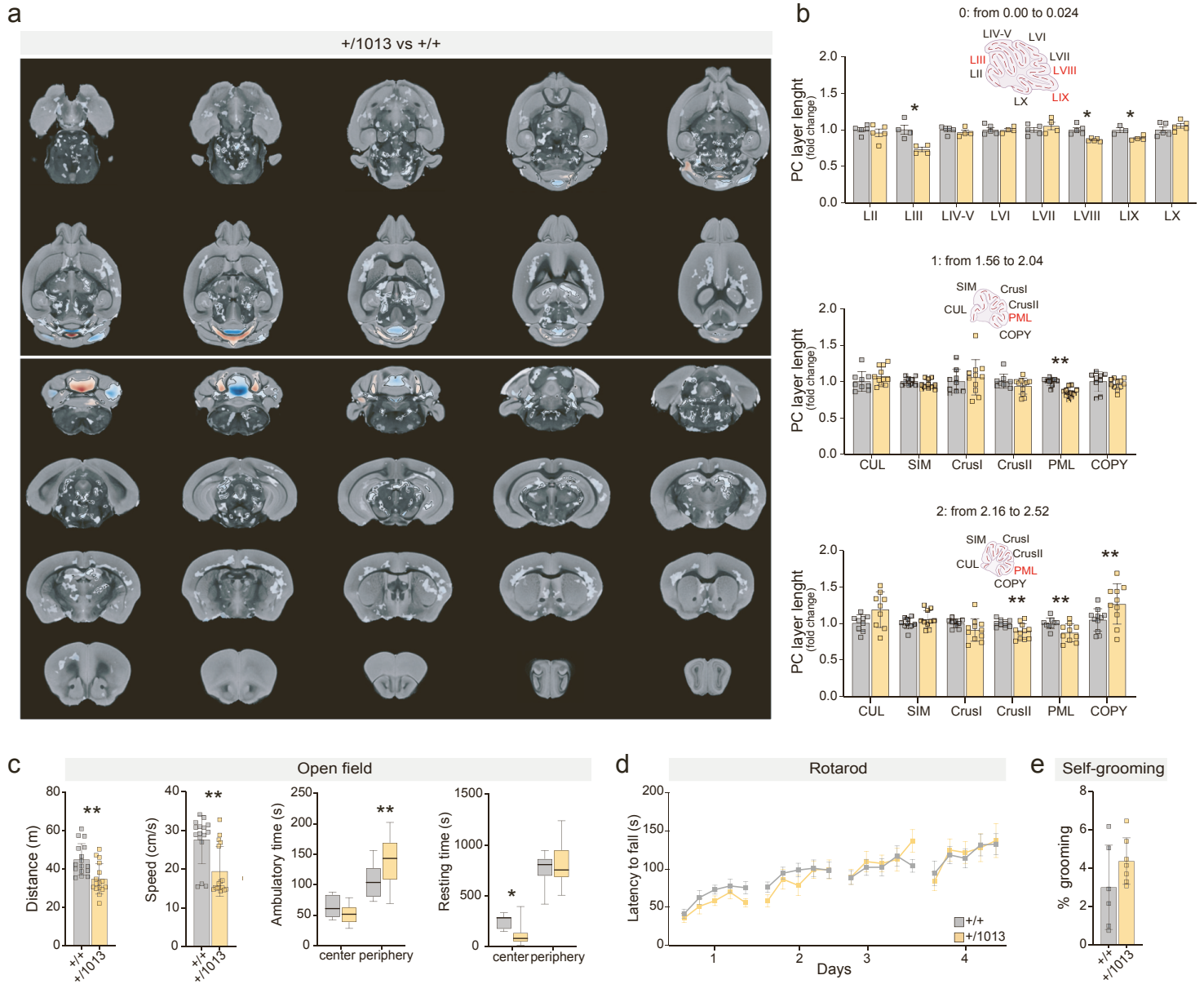


**Supplemental information**

**Neurodevelopmental origins  
of structural and psychomotor defects  
in CXCR4-linked primary immunodeficiency**

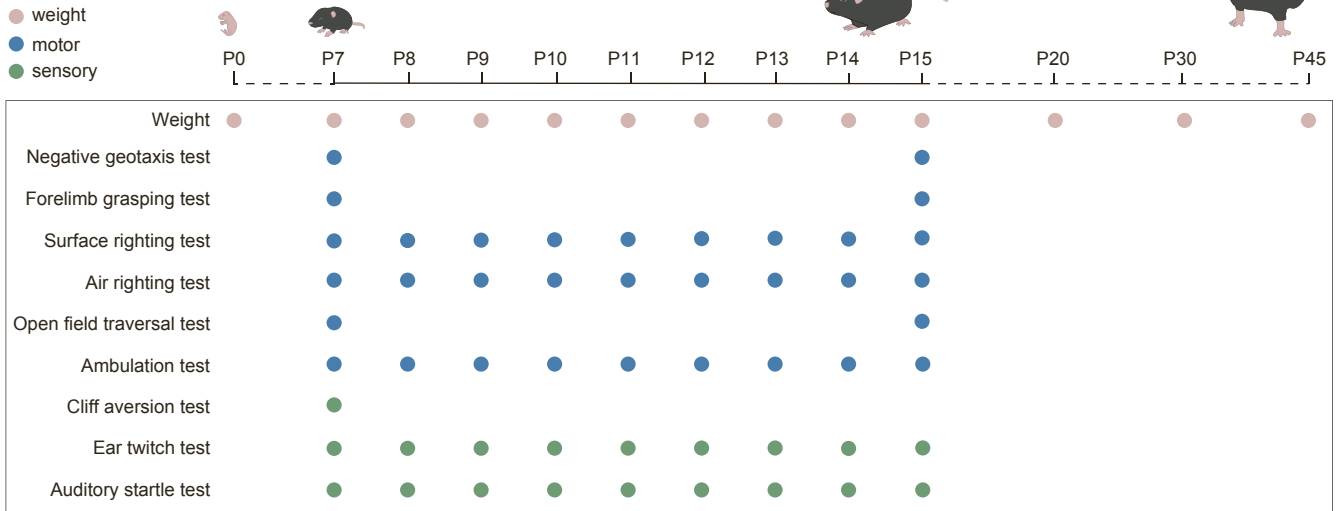
**Giulia Demenego, Sara Mancinelli, Antonella Borreca, Rosalba Olga Proce, Vanessa Aragona, Matteo Miotto, Marco Cremonesi, Laura Zucchelli, Irene Corradini, Eugene Kim, Katarina Ilic, Edoardo Fraviga, Luca Pellegrino, Raffaele Badolato, Roberto Rusconi, Davide Pozzi, Marinos Kallikourdis, Diana Cash, Michela Matteoli, and Simona Lodato**



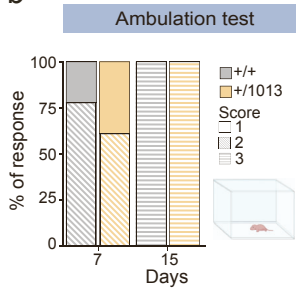


# Demeneo et al., Supplementary Figure 3

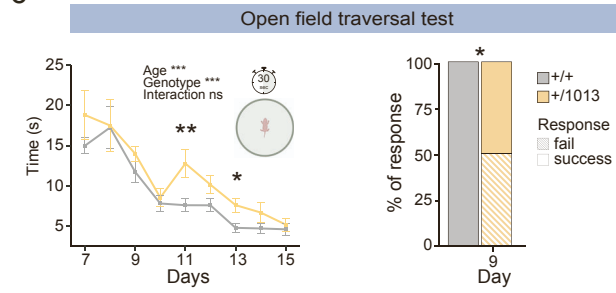
a



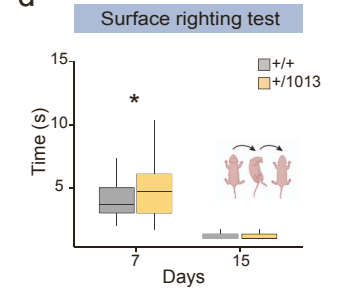
b



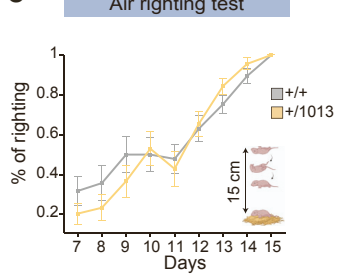
c



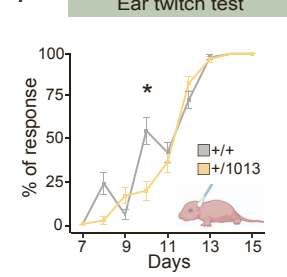
d



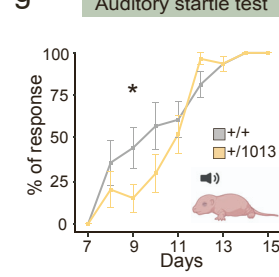
e



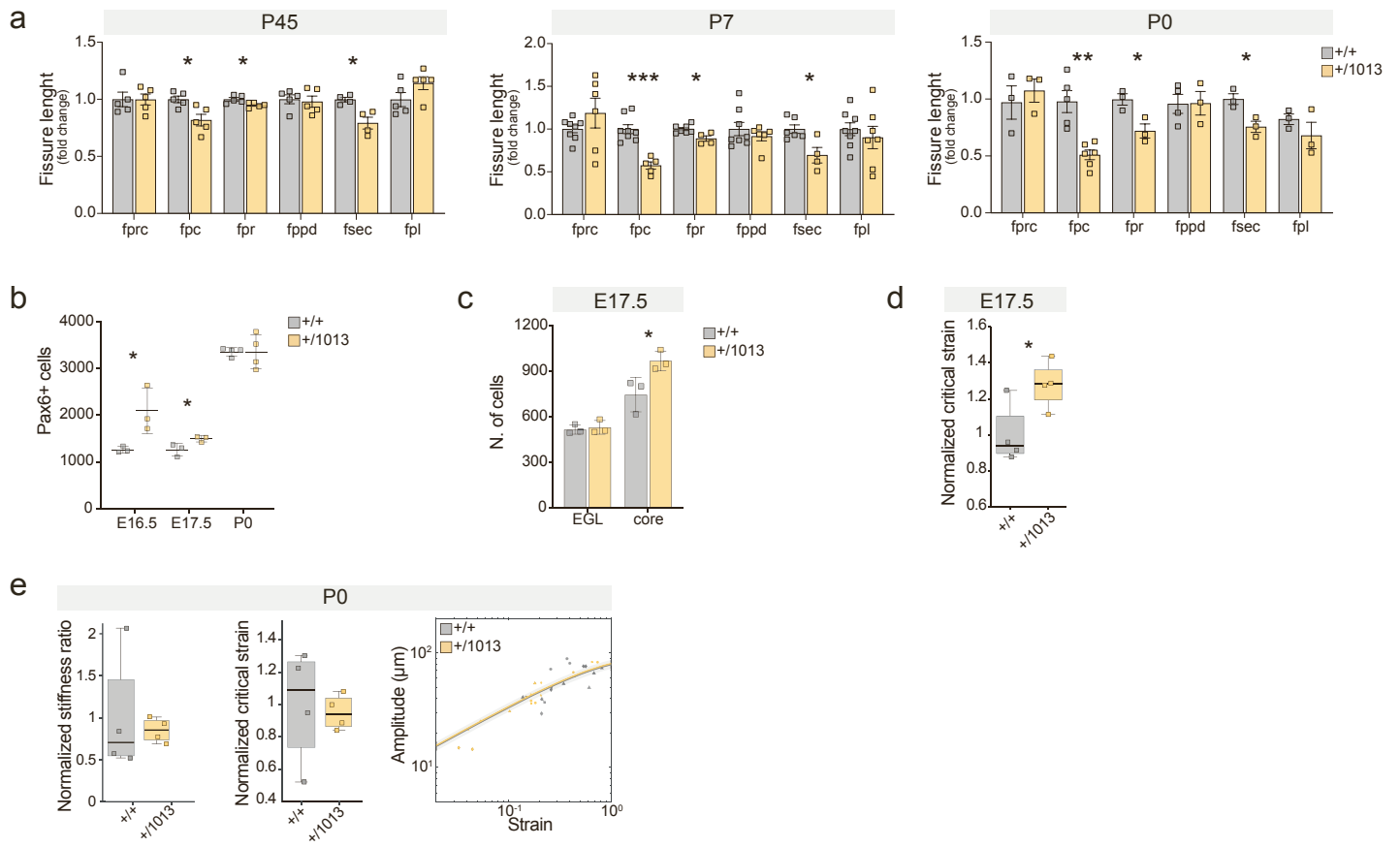
f



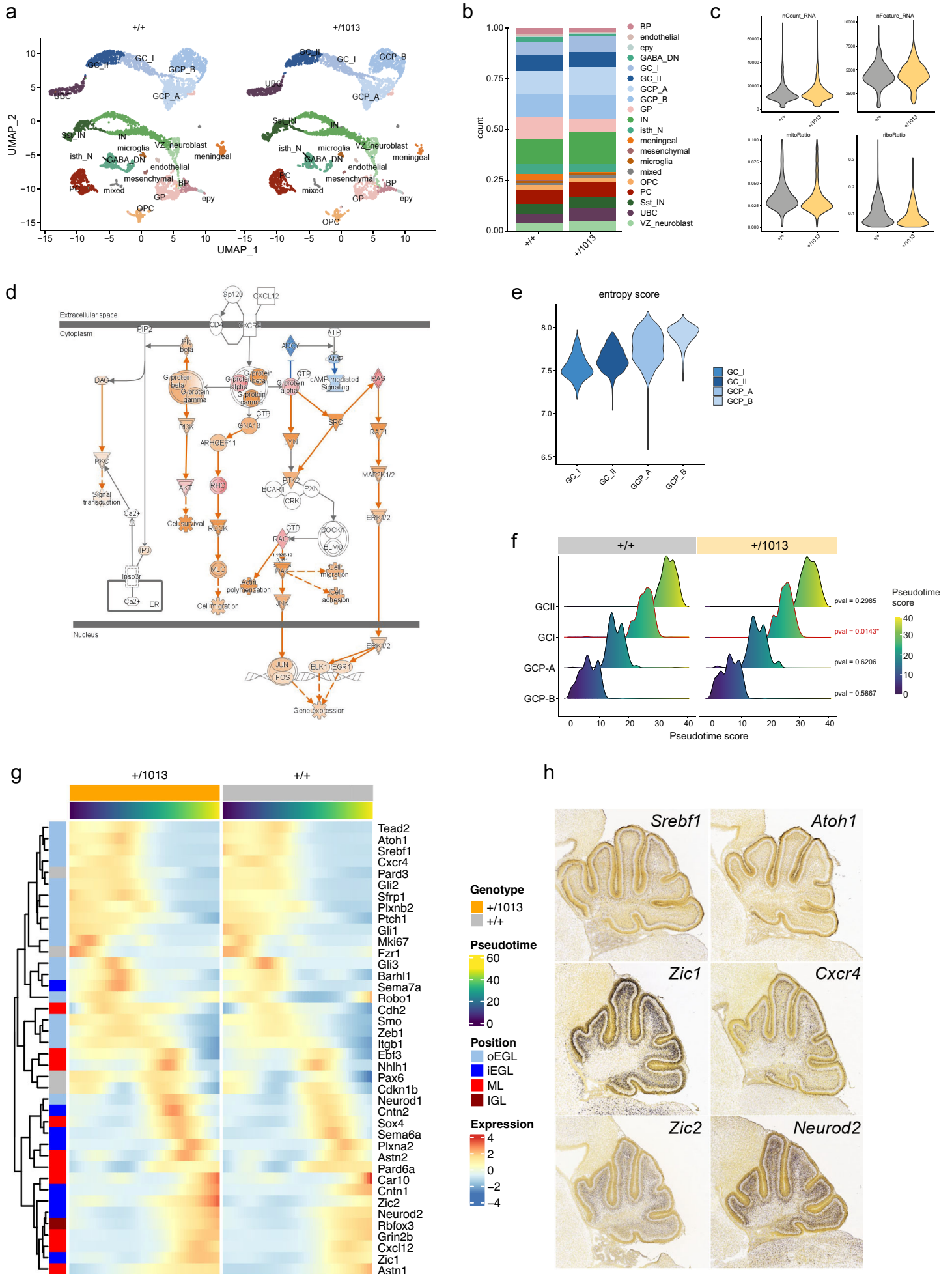
g



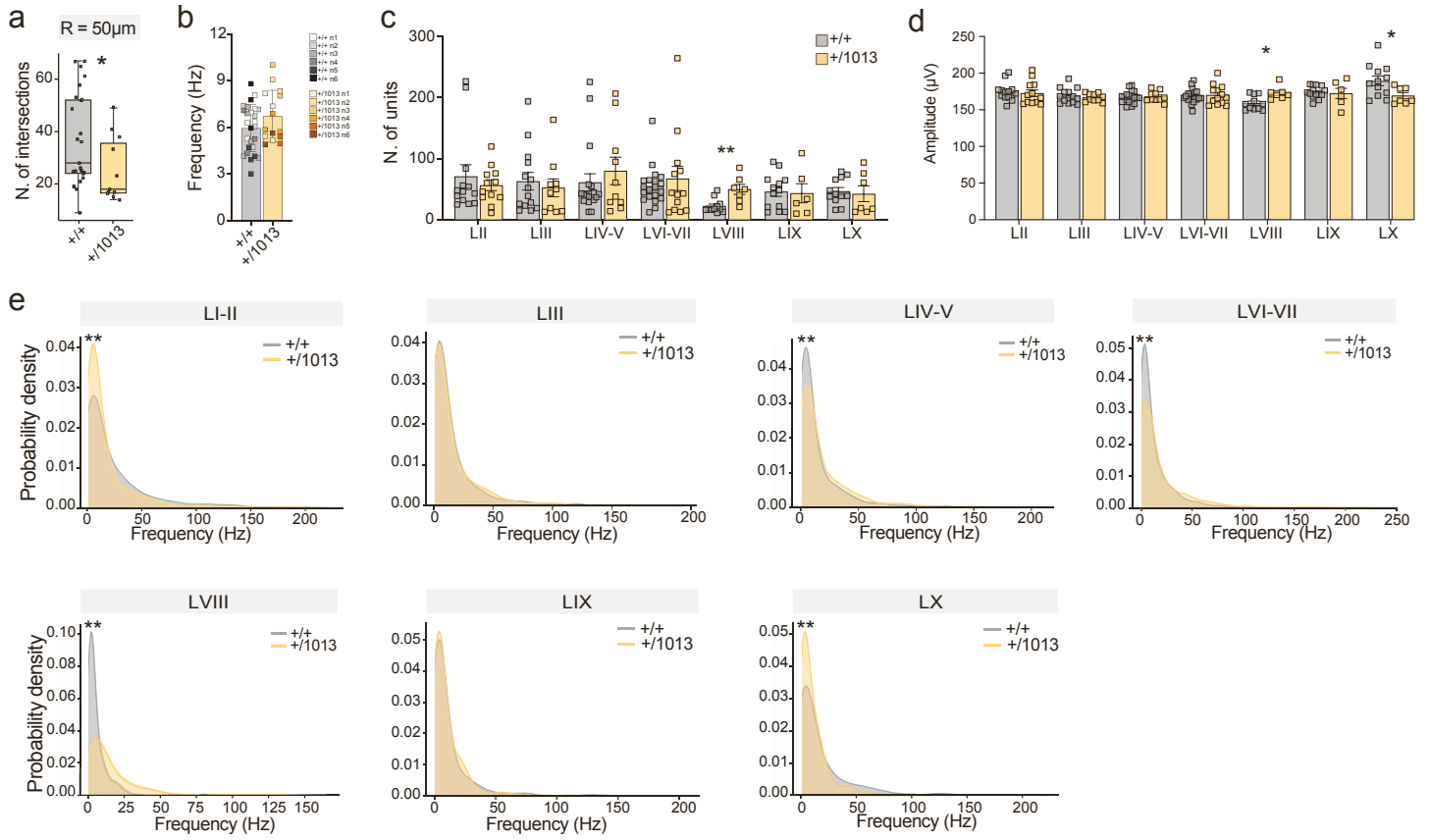
# Demeneo et al., Supplementary Figure 4

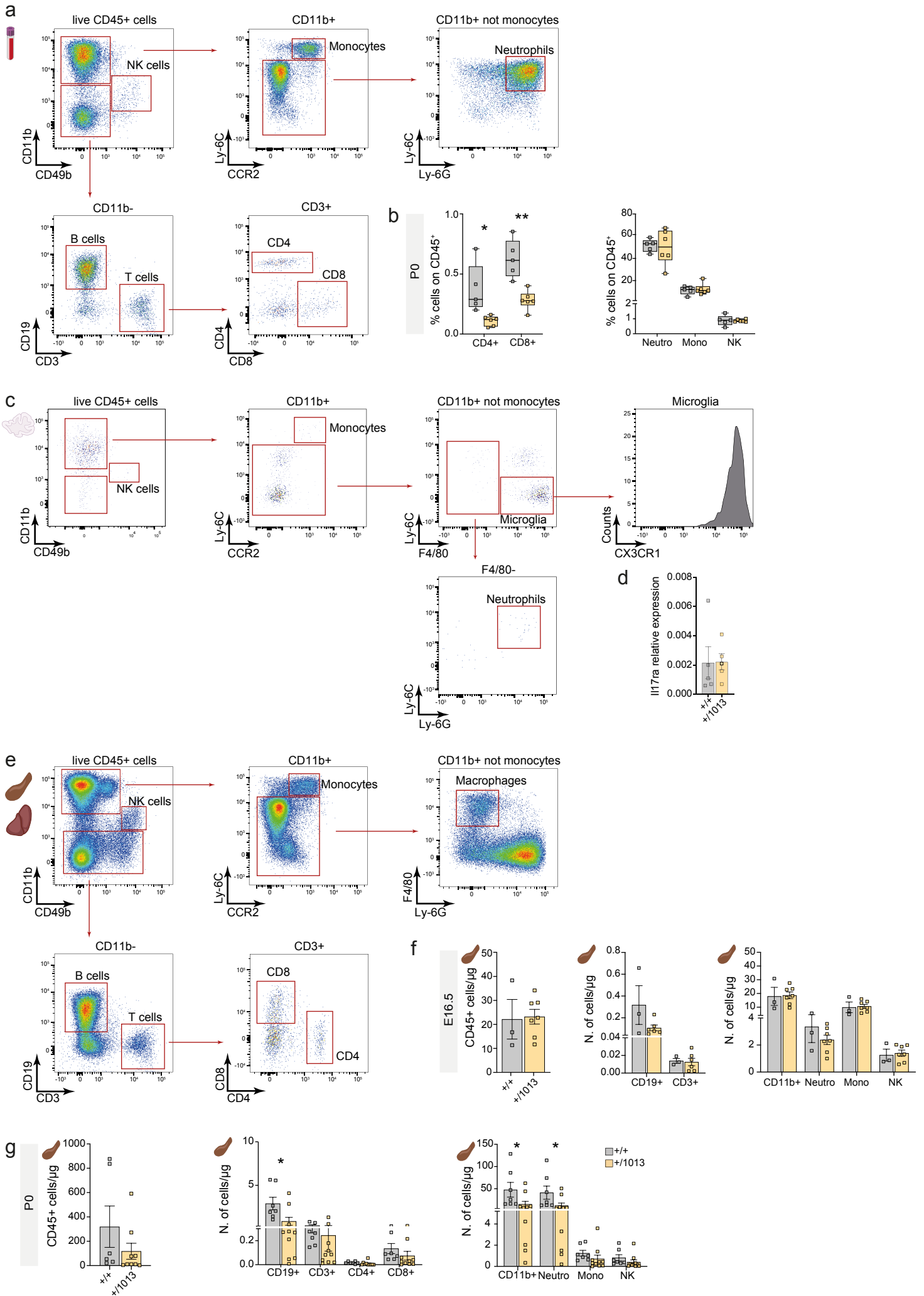


Demeneo et al., Supplementary Figure 5



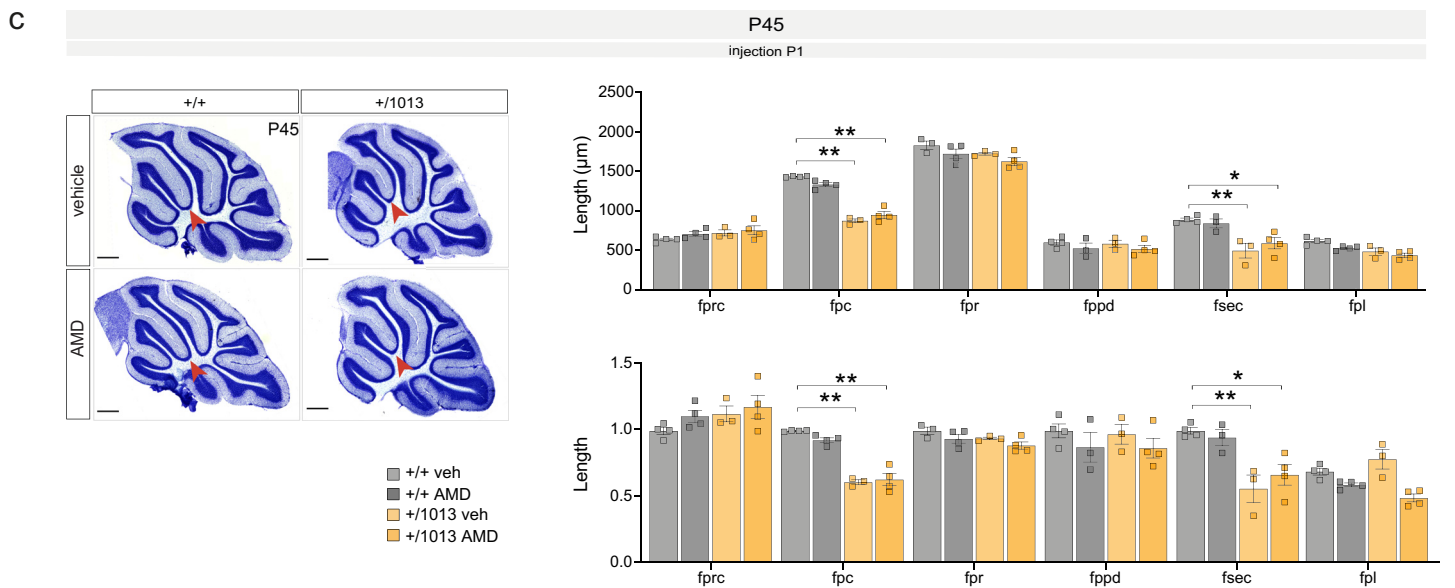
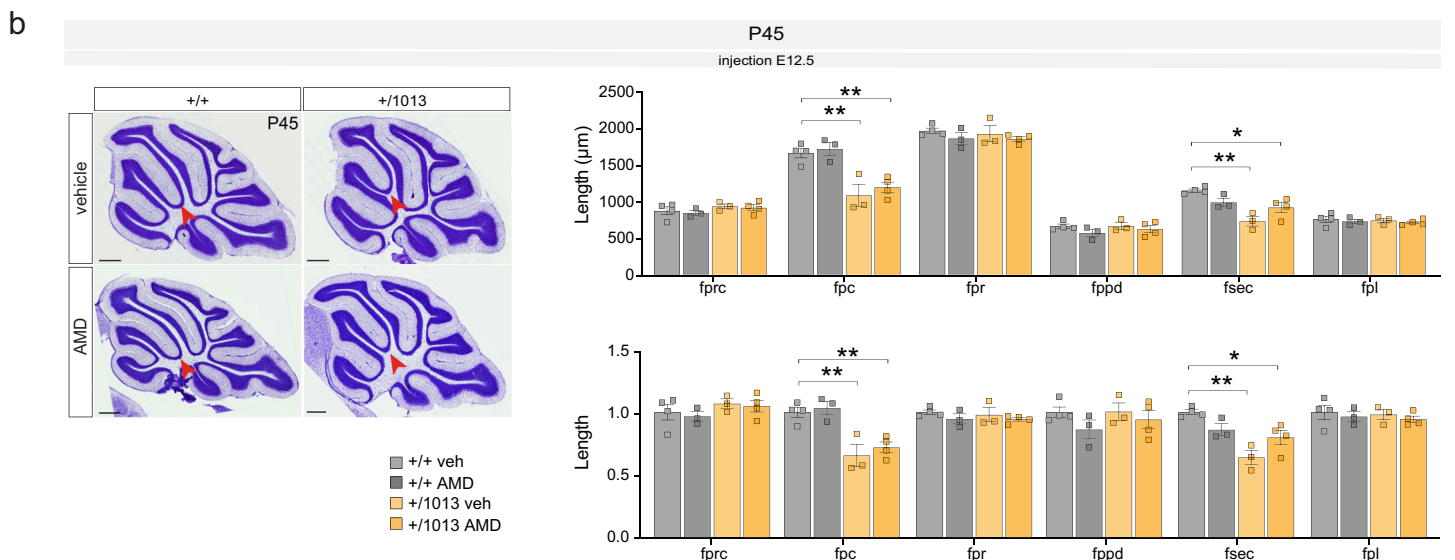
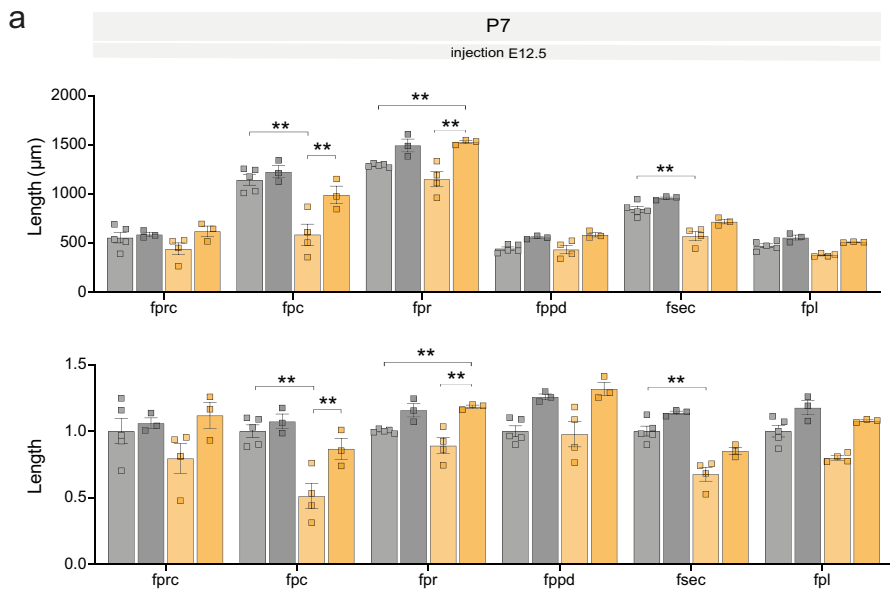
Demeneo et al., Supplementary Figure 6







# Demeneo et al., Supplementary Figure 8



## Supplemental Figure legends

### **Figure S1**

**IEI-associated gene expression in human brain tissues. Related to Figure 1.** (a) Heatmap showing scaled expression of IEI-genes in human brain tissues at different prenatal, postnatal and adult stages. (b) Box plots of average scaled expression of genes showing tissue-specific expression patterns. (c) UMAP colored by cell type of single nuclei derived from healthy donor cerebella from 7 pcw to adulthood<sup>66</sup>. (d) UMAP showing single nuclei colored by developmental stages, from 7 pcw to adulthood. (e) UMAP showing single nuclei colored by lineage (glial, neuronal, vascular and immune) from 7 pcw to adulthood. (f) Dot plot showing subtype-specific expression of selected IEI genes.

Abbreviations: pcw, post-conceptional weeks; mo, months; yrs, years; PFC, prefrontal cortex; CTX, cortex; HP, hippocampus; CB, cerebellum; STR, striatum; AMY, amygdala; TH, thalamus; GC, granule cells; UBC, unipolar brush cells; Glut-DN, glutamatergic neurons of the deep nuclei; Isth-N, isthmic neurons; Norad-N, noradrenergic neurons; GABA-N, GABAergic neurons; IN, interneurons; NPC-NTZ, neuronal precursor cells of the nuclear transitory zone; NPC-VZ, neuronal precursor cells of the ventricular zone; GCP/UBCP, granule cell progenitors/unipolar brush cells progenitors; GCP, granule cell progenitors; APC/OPC, astrocyte progenitor cells/oligodendrocyte progenitor cells; APC, astrocyte progenitor cells; OPC, astrocyte progenitor cells; Astro, astrocytes; BG, Bergmann glia; Oligo, oligodendrocytes; CNS-macroph, central nervous system macrophages; Meningeal-macroph, meningeal macrophages; VC, vascular cells.

### **Figure S2**

**WHIM mice show cerebellar alterations and anxiety-like behavioral phenotypes. Related to Figure 2.** (a) Voxel-wise comparison of cerebellar brain volumes showing gross morphological abnormalities in P45 *Cxcr4*<sup>+/-1013</sup> mice with respect to controls on the horizontal and coronal planes. Red: WHIM larger than WT; blue: WHIM smaller than WT; black contours: regions where FWE-corrected \*p < 0.05; n > 10 animals per condition. (b) Schematic of mouse cerebellum and bar plots and sagittal cerebellar sections at different interaural levels in the vermis (0: 0.00 - 0.24) and hemisphere (1: 1.56 - 2.04; 2: 2.16 - 2.52) showing the length of the PCL length of cerebellar lobules as a fold change. Multiple *t*-test, \*p < 0.05, \*\*p < 0.01; n > 4 animals per condition. (c)

Bar plots showing the distance travelled and speed by control and *Cxcr4*<sup>+/-1013</sup> mice in the open field test. Student's *t*-test, Mann Whitney test, \*\**p* < 0.01; *n* < 16 animals per condition. Box plots showing the ambulatory time (s) and the resting time (s) in the center and periphery of the arena in the open field test. One-way ANOVA, \**p* < 0.05; *n* > 16 animals per condition. **(d)** Line plot indicating the latency to fall (s) from the accelerating rotarod. Two-way ANOVA, \**p* < 0.05; *n* = 11 animals per condition. **(e)** Bar plot indicating the percentage of time spent self-grooming by WHIM and control mice. Student's *t*-test, \**p* < 0.05; *n* > 6 animals per condition.

### **Figure S3**

**WHIM behavioral defects have a developmental origin. Related to Figure 2.** **(a)** Schematic of the developmental milestones performed and experimental time points. **(b)** Stacked bar plot showing the score WHIM and control pups obtain during ambulation test. Multiple *t*-test, \**p* < 0.05; *n* > 30 animals per condition. **(c)** Line plot showing the time *Cxcr4*<sup>+/-1013</sup> and control pups take to walk outside the circle and bar plot showing the number of pups succeeding within 30 seconds in the open field traversal test. Multiple *t*-test, \**p* < 0.05; *n* > 14 animals per condition. **(d)** Box plot showing the time WHIM and control pups take to turn upside down in the surface righting test. Multiple *t*-test, \**p* < 0.05; *n* > 30 animals per condition. **(e)** Line plot showing the percentage of righting *Cxcr4*<sup>+/-1013</sup> and control pups in the air righting test. Multiple *t*-test, \**p* < 0.05; *n* > 4 animals per condition. **(f)** Line plot showing the percentage of response to sensory stimulus in the ear twitch test. Multiple *t*-test, \**p* < 0.05, \*\**p* < 0.01; *n* > 4 animals per condition. **(g)** Line plot showing the percentage of response to auditory stimulus. Multiple *t*-test, \**p* < 0.05, \*\**p* < 0.01; *n* > 4 animals per condition.

### **Figure S4**

**The cerebellar lobulation process is affected in WHIM mutants. Related to Figure 3.** **(a)** Bar plots showing the length of cerebellar fissures as a fold change. Multiple *t*-test, \**p* < 0.05, \*\**p* < 0.01; *n* > 4 animals per condition. **(b)** Dot plot showing the number of Pax6<sup>+</sup> cells in *Cxcr4*<sup>+/-1013</sup> and control cerebella at E16.5, E17.5, P0. Multiple *t*-test, \**p* < 0.05; *n* > 3 animals per condition. **(c)** Bar plot showing the number of Pax6<sup>+</sup> cells in *Cxcr4*<sup>+/-1013</sup> and control EGL and cerebellar core at E17.5. Multiple *t*-test, \**p* < 0.05; *n* = 3 animals per condition. **(d)** Box plot showing an increased normalized critical strain in WHIM cerebellum at E17.5. Student *t*-test, \**p* < 0.05; *n* > 3 animals

per condition (e) Box plot showing unaltered stiffness ratio and normalized critical strain in *Cxcr4*<sup>+/1013</sup> cerebellum at P0. High deformation wrinkling models (solid lines) showing a slight decrease in amplitude in WHIM cerebellum at P0. Student t-test; n > 3 animals per condition.

### Figure S5

**Single-cell sequencing of developing WHIM and control cerebellar lobules. Related to Figure 4 and Figure 5.** (a) UMAP plot of control and *Cxcr4*<sup>+/1013</sup> cerebella colored by cell type. (b) Stacked bar plots showing proportion of 19 distinct cell types between genotypes. (c) Violin plots showing the distribution of number of UMIs per cell, number of genes per cell, mitochondrial and ribosomal genes ratios in of control and *Cxcr4*<sup>+/1013</sup> cerebellar samples. (d) Ingenuity Pathway Analysis (IPA) revealed significant upregulation of *Cxcr4* signaling pathway components in cerebellar progenitors. (e) Violin plot showing the entropy score/cell type. (f) Density plot colored by pseudotime score value for each cell type split by genotype. (g) Pseudotime heatmap of genes associated with cortical cerebellar layers (left annotation bars) along the granule cell lineage split by genotype. (h) Representative sagittal *in-situ* images from Allen Brain Atlas showing the expression of granule lineage markers at P4.

Abbreviations: PC, Purkinje cells; UBC, unipolar brush cells; OPC, oligodendrocyte precursor cells; Sst-IN, Somatostatin<sup>+</sup> interneurons; IN, interneurons; VZ\_neuroblast, ventricular zone neuroblast; isth-N, isthmus neurons; GC\_I/II, granule cells; GCP\_A/B, granule cell precursor; epy, ependymal precursors; BP, bipotent progenitor; GP, gliogenic progenitor; GABA\_DN, GABAergic neurons of the deep nuclei; nCount\_RNA, number of UMIs per cell; nFeature\_RNA, number of genes per cell; mitoRatio, mitochondrial genes ratio; riboRatio, ribosomal genes ratio.

### Figure S6

***Cxcr4* mutation impacts PC morphology and function. Related to Figure 6.** (a) Box plot showing the number of intersections in WHIM PC compared to controls at radius = 50μm. Student's *t*-test, \*p > 0.05; n > 7 cells per condition. (b) MFR analysis calculated in the entire cerebellum in *Cxcr4*<sup>+/1013</sup> and controls. (c) Bar plot showing the number of active units in each lobe of *Cxcr4*<sup>+/1013</sup> and controls. Mann-Whitney test, \*p > 0.05; n > 6 animals per condition. (d) Bar plot showing quantitative analysis of amplitude recorded in each lobe. Dots show the number of analyzed slices. Mann-Whitney test, \*p < 0.05; n > 6 animals per condition. (e) Probability

density functions of single lobe frequency in *Cxcr4*<sup>+/-1013</sup> and controls. Kernel density estimation, \*\*p < 0.01; n > 6 animals per condition.

### Figure S7

**WHIM immunological phenotype is evident as early as birth. Related to Figure 7.** (a) Representative flow cytometry gating strategy for identification of NK cells (CD11b<sup>low</sup>CD49b<sup>+</sup>), monocytes (CD11b<sup>+</sup>Ly6C<sup>+</sup>), neutrophils (CD11b<sup>+</sup>Ly6C<sup>+</sup>Ly6G<sup>+</sup>), B cells (CD11b<sup>-</sup>CD19<sup>+</sup>CD3<sup>-</sup>) and T cells (CD11b<sup>-</sup>CD19<sup>-</sup>CD3<sup>+</sup>CD4<sup>+</sup>, CD11b<sup>-</sup>CD19<sup>-</sup>CD3<sup>+</sup>CD8<sup>+</sup>) isolated from the blood of P0 WHIM and control pups. (b) Box plots showing the percentage of circulating immune cell subsets in P0 WHIM blood analyzed by FACS. Student's *t*-test, \*p < 0.05; n > 4 animals per condition. (c) Representative flow cytometry gating strategy for identification of NK cells (CD11b<sup>low</sup>CD49b<sup>+</sup>), monocytes (CD11b<sup>+</sup>Ly6C<sup>+</sup>), microglia (CD11b<sup>+</sup>Ly6C<sup>-</sup>F4/80<sup>+</sup>CX3CR1<sup>+</sup>) and neutrophils (CD11b<sup>+</sup>F4/80<sup>+</sup>Ly6C<sup>+</sup>Ly6G<sup>+</sup>) isolated from the cerebellum of P0 *Cxcr4*<sup>+/-1013</sup> and control pups. (d) Bar plot showing the relative expression of *Il17ra* in adult WHIM cerebellum quantified by RT-qPCR, normalized on *Gadph* expression. (e) Representative flow cytometry gating strategy for identification of NK cells (CD11b<sup>low</sup>CD49b<sup>+</sup>), monocytes (CD11b<sup>+</sup>Ly6C<sup>+</sup>), macrophages (CD11b<sup>+</sup>Ly6G<sup>+</sup>F4/80<sup>+</sup>), B cells (CD11b<sup>-</sup>CD19<sup>+</sup>CD3<sup>-</sup>) and T cells (CD11b<sup>-</sup>CD19<sup>-</sup>CD3<sup>+</sup>CD4<sup>+</sup>, CD11b<sup>-</sup>CD19<sup>-</sup>CD3<sup>+</sup>CD8<sup>+</sup>) isolated from the liver (E16.5) and spleen (E16.5 and P0) of *Cxcr4*<sup>+/-1013</sup> and control pups. (f) Bar plot showing different immune cell subsets in E16.5 WHIM spleen. Student's *t*-test, \*p < 0.05; n > 4 animals per condition. (g) Bar plots showing different immune cell subsets in P0 WHIM spleen. Student's *t*-test, \*p < 0.05; n > 4 animals per condition. Abbreviations: Neutro, neutrophils; Mono, monocytes; Macro, macrophages; NK, natural killer cells.

### Figure S8

**WHIM behavioral and structural alterations can be rescued at early developmental stages. Related to Figure 8.** (a) Bar plots showing fissure length (μm or fold change) in P7 WHIM and control cerebella upon AMD3100 or vehicle injection at E12.5. Multiple t-test, \*p < 0.05, \*\*p < 0.01; n > 3 animals per condition. (b) Representative sagittal Nissl sections of WHIM and control cerebella at P45 upon AMD3100 or vehicle injection at E12.5 and bar plots showing fissure length (μm or fold change). Scale bar = 500 μm. Multiple t-test, \*p < 0.05, \*\*p < 0.01; n > 3 animals per

condition. (c) Representative sagittal Nissl sections of WHIM and control cerebella at P45 upon AMD3100 or vehicle injection at P1 and bar plots showing fissure length ( $\mu\text{m}$  or fold change). Multiple t-test,  $*p < 0.05$ ,  $**p < 0.01$ ;  $n > 3$  animals per condition.

Abbreviations: AMD, AMD3100; veh, vehicle; fprc, precentral fissure; fpc, preculminary fissure; fpr, primary fissure; fppd, prepyramidal fissure; fsec, secondary fissure; fpl, posterolateral fissure.